Copper-Phosphido Catalysis: Enantioselective Addition of Phosphines to Cyclopropenes

Brian S. Daniels,[‡] Xintong Hou,[‡] Stephanie A. Corio, Lindsey M. Weissman, Vy M. Dong,[*] Jennifer S. Hirschi,[*] Shaozhen Nie[*]

Department of Chemistry, University of California, Irvine, Irvine, California 92697, United States

Department of Chemistry, Binghamton University, Binghamton, New York 13902, United States

Department of Medicinal Chemistry, GSK, Collegeville, Pennsylvania 19426, United States

ABSTRACT: We describe a copper catalyst that promotes the addition of phosphines to cyclopropenes at ambient temperature. A range of cyclopropylphosphines bearing different steric and electronic properties can now be accessed in high yields and enantioselectivities. Enrichment of phosphorus stereocenters is also demonstrated via a DyKAT process. A combined experimental and theoretical mechanistic study supports an elementary step featuring insertion of a Cu(I)-phosphido into a carbon-carbon double bond. Density functional theory calculations reveal migratory insertion as the rate- and stereo-determining step, followed by a *syn*-protodemetalation.

By inventing strategies to forge C–P bonds, chemists provide entrance to organophosphorous architectures for versatile applications in medicine and catalysis.[1] Among these architectures, the cyclopropyl phosphine motif garners attention because of its distinctive steric and electronic attributes. For example, a cyclic analogue of fosmidomycin shows enhanced antibiotic activity against E. coli, presumably due to restricted rotation.[2] In the realm of catalysis, Takasago's cyclopropyl phosphine ligand, cBRIDP outperforms its vBRIDP in Suzuki-Miyaura cross coupling.[3] Considering ways to construct cyclopropyl phosphines, we focused on hydrophosphination: the direct addition of a P–H bond across a C–C multiple bond.[4] Hydrophosphination represents an attractive and atom-economical platform[5] for controlled synthesis of molecules with stereogenic carbon and/or phosphorous atoms. While progress has been made,[6] stereoselective methods remain rare beyond use of alkynes,[7] oxa-bicycles,[8] and Michael acceptors.[9] Driven by strain release,[10] cyclopropenes show high reactivity,[11,12] and the hydrofunctionalization of cyclopropenes has enabled a direct access to a diverse range of enantiomerically enriched rings.[12] In this report, we disclose enantioselective Cu-catalyzed hydrophosphination to access a range of cyclopropyl-phosphines at ambient temperature. A unique Cu-phosphido mechanism is supported by both experimental and theoretical studies. We provide insights into ligand trends for selectivity using buried volume analysis.

Organophosphorous partners bearing P–H bonds with a wide range of acidities (pK_a 9.0 to 22.4)[13] can be activated with transition metal catalyts.[14] For secondary phosphines, coordination followed by deprotonation results in a metal-phosphido complex,[9a,9f,9i-k] with high nucleophilicity, and recent studies have revealed impressive versatility of catalytically generated Cu-phosphido complexes.[9e,9g-h,15] Glueck elucidated mechanistic and structural details,[15d,e] while both Glueck and Yin demonstrated catalytic transformations using Cu-phosphidos (Figure 1B).[9g,h] Previous strategies using cyclopropenes to forge C–P bonds focused on Pd catalysis.

A. Cyclopropyl phosphorus-containing molecules

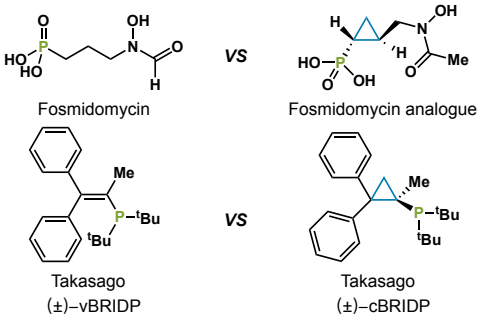

B. State of art in asymmetric Cu-phosphido catalysis.

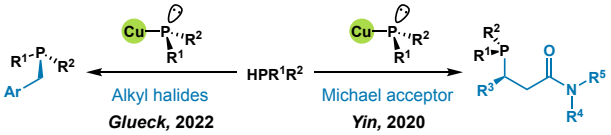

C. Proposed asymmetric hydrophosphination of cyclopropenes.

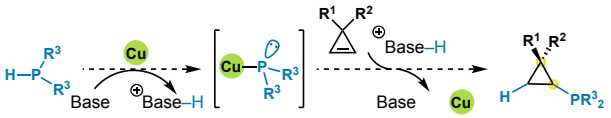

Figure 1. Inspiration of asymmetric hydrophosphination of cyclopropenes.

Both phosphine oxides and phosphites gave ring-opening to afford allylic phosphine oxides and allylic phosphonates, respectively.[16] At the start of our studies, there was only one transformation, using phosphine oxides and cyclopropenes that provided the ring-retained cyclopropyl phosphine product, albeit as a racemic mixture.[14l] Coinciding with our efforts, the Wang group was independently pursuing the enantioselective addition of phosphines to cyclopropenes by Pd-catalysis; their asymmetric version occurs by Pd–H insertion into the cyclopropene.[4h] While promising, the scope is limited strictly to ester-bearing cyclopropenes and requires precious metal.

While precious metals are practical on industrial scales,[17] earth abundant metals are more sustainable and economical, while providing an opportunity to uncover novel and complementary reactivity.[18] As an alternative to Pd–H mechanisms, we imagined a strategy involving Cu-phosphido catalysis. Insertion of a Cu-phosphido into cyclopropenes, followed by protodemetalation, would generate chiral cyclopropyl phosphines (Figure 1C).[15]

Table 1. Ligand effects on asymmetric hydrophosphination of 1a[a]

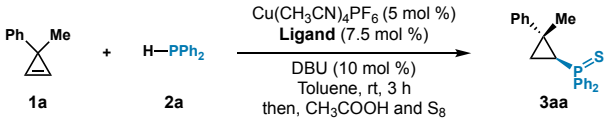

1a 2a 3aa

entry	variations	yield (%)	*er*
1	—	92	98:2
2	without $Cu(CH_3CN)PF_6$	—	—
3	without DBU	—	—
4	no (R,R)-^{i}Pr-DuPhos	77	—
5	6 mol% ((R,R)-^{i}Pr-DuPhos	91	79:21
6	**L1** instead of **L5**	90	85:15
7	**L2** instead of **L5**	82	64:36
8	**L3** instead of **L5**	70	90:10
9	**L4** instead of **L5**	73	92:8

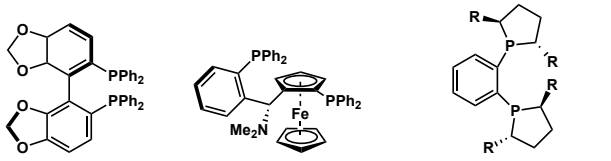

R-SEGPHOS (**L1**) Taniaphos (**L2**) (R,R)-DuPhos
R = Me(**L3**), Et(**L4**), ^{i}Pr(**L5**)

[a]Reaction conditions: **1a** (0.12 mmol), **2a** (0.10 mmol), $Cu(CH_3CN)_4PF_6$ (5.0 mol%), ligand (7.5 mol%), DBU (10 mol%), toluene (0.40 mL), 3 h. Yield determined by GC-FID analysis of the reaction mixture, which was referenced to 1,3,5-trimethoxybenzene as internal standard. Enantioselectivity determined by chiral SFC.

In our initial studies, we surveyed phosphine oxides and found that it was difficult to achieve high enantioselectivity (Table S1). In contrast, diphenyl phosphine (**2a**) gave promising results with Cu. Therefore, we choose diphenyl phosphine (**2a**) and cyclopropene **1a** as model substrates. For the convenience of handling and analysis, the cyclopropyl phosphine products were oxidized with sulfur to generate the corresponding phosphine sulfides. In previous studies using copper catalysis, Yin's group demonstrated the superiority of Taniaphos ligands for the Cu-catalyzed alkylation of secondary phosphines.[9g] However, Taniaphos ligands were ineffective in this cyclopropene hydrophosphination (Table 1, entry 7). Instead, we found the DuPhos ligand family most promising (Table 1, entry 8,9). Higher selectivity was correlated with larger R-substituents on the ligand (92% yield, 98:2 *er*) (*vide infra*). The addition of base is necessary to promote the formation of Cu-phosphido (Table 1, entry 3). With further tuning of the reaction stoichiometry, we developed a convenient and practical protocol for the asymmetric coupling of phosphines and cyclopropenes under Cu catalysis. In parallel, we identified a related protocol using Pd catalysis that is complementary to Wang's. While the Wang group reported that cyclopropene **1a** does not transform under with their standard conditions (5 mol% Pd_2dba_3, 11mol% (R,R)-QuinoxP, 1,4-dioxane, 60 °C),[4g] we found that $Pd(OAc)_2$, in the presence of (R)-SEGPHOS, provides cyclopropyl phosphine **3aa** in 86 % yield with 97:3 *er*.[19] With this Pd condition, we also obtained phenyl ester cyclopropyl phosphine **3la** (84%, 96:4 *er*, >20:1 *dr*) and *p*-chloro phenyl ester cyclopropyl phosphine **3ma** (68%, 94:6 *er,* 9:1 *dr*) by desymmetrizing corresponding cyclopropenes (see SI 2B for details).

Table 2. Hydrophosphination of various cyclopropenes.[a]

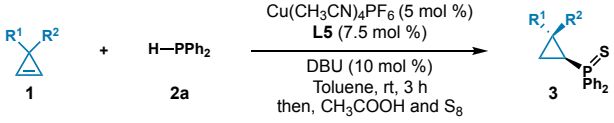

1 2a 3

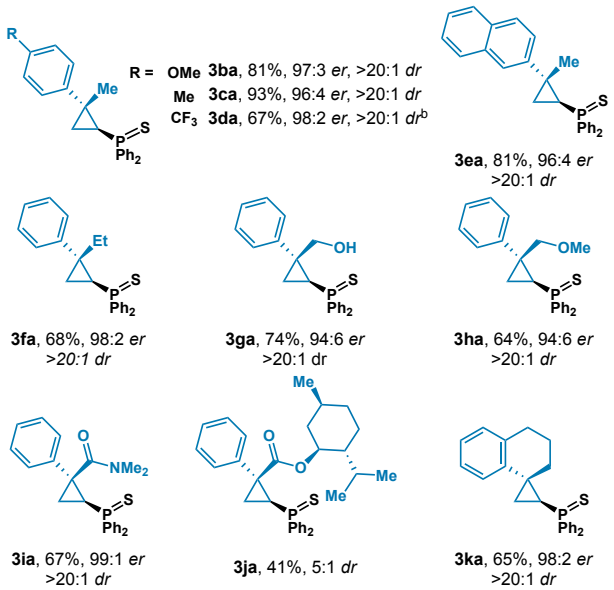

[a]Reaction conditions: **1** (0.12 mmol), **2a** (0.10 mmol), $Cu(CH_3CN)_4PF_6$ (5.0 mol%), ligand (7.5 mol%), DBU (10 mol%), toluene (0.40 mL), 3 h. Isolated yield of **3**. Diastereomeric ratios (*dr*) were determined from ^{1}H NMR analysis of the unpurified reaction mixture. Enantioselectivity determined by chiral SFC. [b]Reaction time is 24 hours, see SI for details.

With this Cu catalyzed transformation, we achieved a scope of 10 unique cyclopropenes with different functionalities,

electronics and sterics as summarized in Table 2. High yields (81-93%) and stereoselectivities (96:4-97:3 *er*) are observed for cyclopropenes bearing electron-rich aromatic rings (**3ba**, **3ca**). Electron-poor aromatic ring (**3da**) gives good stereoselectivities (>20:1 *dr*, 98:2 *er*) and moderate yield (67%). Substituents on the cyclopropene can be replaced with bulkier naphthyl (**3ea**) and ethyl groups (**3fa**). Cyclopropenes with alcohol (**3ga**) and methyl ether (**3ha**) substituents undergo the transformation with moderate yields (64-74%) and high stereoselectivities (>20:1 *dr*, 94:6 *er*). In addition, amide substituted cyclopropene (**3ia**) undergoes hydrophosphination (67% yield, >20:1 *dr*, 99:1 *er*), and menthol ester cyclopropene (**3ja**) gave moderate diastereoselectivity (5:1 *dr*). With this transformation, we also successfully prepared spirocyclic phosphine **3ka**.[20,21]

Table 3. Hydrophosphination of **1a** with various phosphines.[a]

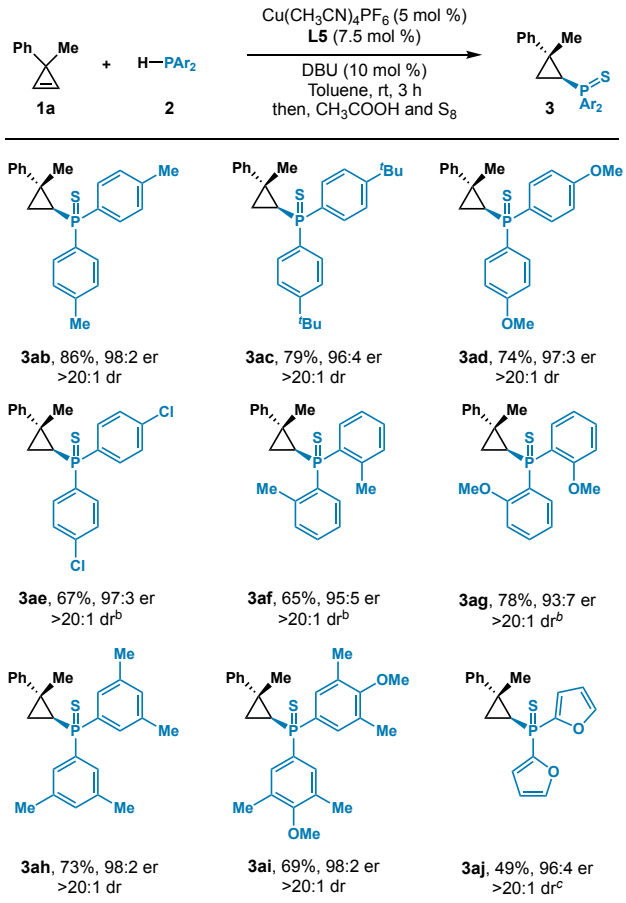

[a]Reaction conditions: **1** (0.12 mmol), **2a** (0.10 mmol), $Cu(CH_3CN)_4PF_6$ (5.0 mol%), ligand (7.5 mol%), DBU (10 mol%), toluene (0.40 mL), 3 h. Isolated yield of **3**. Diastereomeric ratios (*dr*) were determined from ^1H NMR analysis of the unpurified reaction mixture. Enantioselectivity determined by chiral SFC. [b]Reaction performed for 12 hours. [c]Reaction performed at 80 °C for 12 hours.

Our method encompasses a range of phosphine nucleophiles as shown in Table 3. Phosphines bearing electron donating Me, ^{t}Bu, and OMe groups at the para position (**3ab**, **3ac**, **3ad**) add to cyclopropenes (74-86%) with high enantioselectivities (96:4-98:2 *er*). Electron poor phosphines are well-tolerated (**3ae**). Even phosphines with ortho substituted (**3af**, **3ag**), 3,5-substituted (**3ah**) and 3,4,5-substituted aromatic rings (**3ai**) transform in 65-78% yield and high enantioselectvities (93:7-98:2 *er*). This method tolerates heterocyclic phosphines, such as 2-furyl **2j**, which gives **3aj** (49% yield, 96:4 *er*) at elevated temperature (80 °C, 12 hours).

Based on literature precedent[9g,15d-e] and our own observations, we propose the general catalytic cycle in Figure 2A. Initially, $Cu(CH_3CN)_4PF_6$ binds to (*R*,*R*)-^{i}Pr-DuPhos to generate a mono(chelate) species **4** followed by the mono-coordination of phosphine (**2**) and deprotonation to generate Cu-phosphido complex **5**. The novel step in the cycle involves addition of Cu-phosphido intermediate (**5**) to the cyclopropene (**1a**). We imagined that **5** could undergo either direct nucleophilic attack[22] or insertion into the cyclopropene π-bond.[23] Lastly, elimination of the copper catalyst regenerates **4** and releases cyclopropyl phosphine **3** to complete the catalytic cycle.

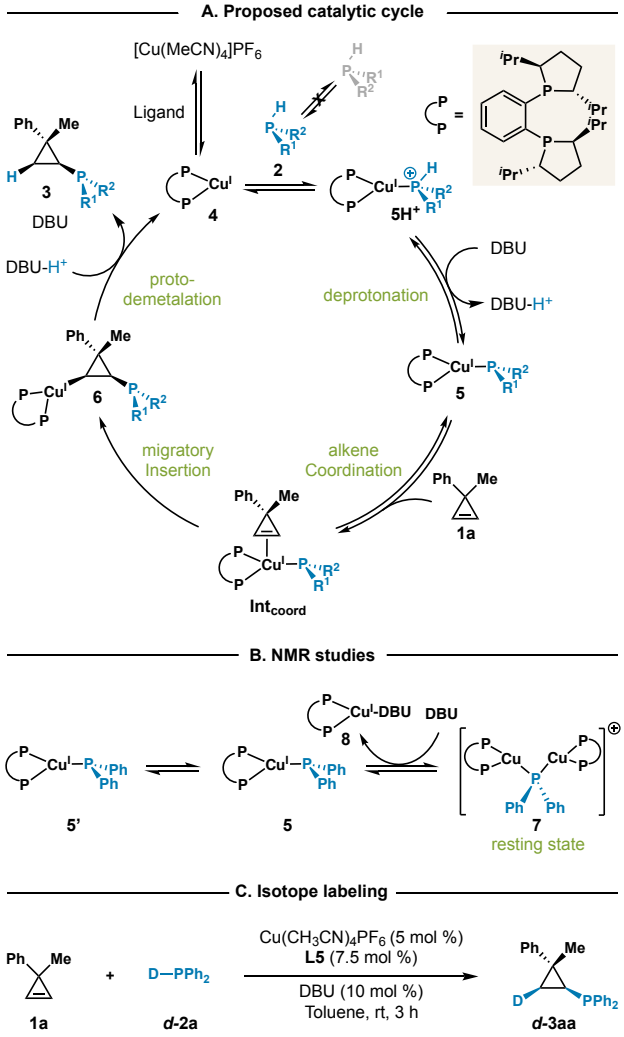

Figure 2. Proposed Mechanism and Experimental Studies

To investigate our proposed mechanism, we performed a series of experiments. These experiments were performed in THF which provided a more homogeneous solution as compared to toluene. First, we obtained the rate law by variable time normalization analysis.[24] We observed a first order dependance on the DBU concentration and a fractional order dependance on the copper catalyst concentration. In

Yin's related study, the addition of a base (e.g., Barton's base) to a mixture of $Cu(CH_3CN)_4PF_6$, bidentate phosphine ligand,[9l] and secondary phosphine results in a complicated and uncharacterizable mixture. In stark contrast, we found that addition of various bases (e.g., DBU, ^{t}BuOK, and Et_3N) to a mixture of $Cu(CH_3CN)_4PF_6$, (*R*,*R*)-^{i}Pr-DuPhos, and diphenylphosphine results in immediate and selective formation of a new species on the basis of ^{31}P NMR. This species was isolated and further characterized by ^{1}H NMR, ^{31}P NMR and mass spec analysis and determined to be a Cu-phosphido dimer **7** (Figure 2B). In this dimer, the lone pair of the X-type phosphido ligand of **5** acts as an L-type ligand to form a η^2 bridge to another unit of Cu-DuPhos mono-chelate **4** via a three-center four-electron bond. We propose this species to be the catalyst resting state. In line with this observation, our kinetics studies, and similar observations made by Appel and coworkers while studying copper hydride catalysis,[25] we propose the DBU acts as not only a base but also an L-type ligand. The DBU undergoes ligand substitution with the dimeric resting state **7** to liberate the catalytically active monomeric Cu-phosphido **5**. This hypothesis is further supported by ^{31}P NMR studies which reveal decomposition of the dimer **7** with concomitant formation of an unidentified species in the presence of large excesses of DBU. Performing the transformation with isotopically labelled *d*-**2a** revealed that the hydrophosphination proceeds via a formal syn-addition of the P–D bond across the cyclopropene double bond (Figure 2C).[26]

With this mechanism in mind, we examined the possibility of setting a phosphorus stereocenter via a dynamic kinetic asymmetric transformation (DyKAT).[27] As outlined in the proposed mechanism, pyramidal inversion of the secondary phosphine is impractically slow at room temperature while epimerization of Cu-phosphido **5** with **5'** occurs rapidly.[15c-e,28] We subjected unsymmetrically substituted phosphine **2k** to the reaction conditions to test this hypothesis and observed a 3:1 *dr* for the cyclopropyl phosphine products and an *er* of 96:4 and 88:12 for the major and minor diastereomer, respectively, (Scheme 1). Based on our prior results, we assume effective desymmetrization of the cyclopropene occurs with relatively low control over the configuration of the phosphorus stereocenter; these results are in line with a recent report from Glueck using a similar catalyst for asymmetric alkylation of secondary phosphines.[15d,15e] On the basis of ^{31}P NMR studies, Glueck and coworkers were able to observe both Cu-phosphido diastereomers and measure the relative diastereomeric ratio (3:1 *dr*). They found that this Cu-phosphido diastereoselectivity correlates to the observed enantioselectivity for the alkylation step (3:1 *er*). In our case, we observe a single dimeric resting state, which thwarted attempts at a similar analysis for the diastereoselectivity of Cu-phoshido formation.

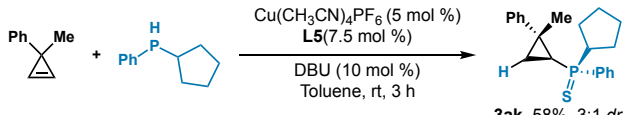

1a **rac-2k** **3ak**, 58%, 3:1 *dr*, 96:4/88:12 *er*

Scheme 1. Dynamic kinetic asymmetric transformation.

To support the proposed mechanism and pursue more elusive details for the enantioselective hydrophosphination of cyclopropenes, we performed a density functional theory (DFT) analysis on the title reaction of 3-methyl-3-phenylcyclopropene (**1a**) and diphenylphosphine (**2a**) catalyzed by Cu-^{i}Pr-Duphos complex (**4**). DFT computations were performed utilizing ωB97XD/def2TZVP PCM(toluene)// B97D/def-2SVP level of theory as implemented in Gaussian 16.[29-35] Thermal corrections were computed using Grimme's quasi-rigid rotor harmonic oscillator approximation.[36] IRC calculations were performed to confirm that transition structures (TSs) connected minima along the potential energy surface. A thorough exploration of the catalyst conformational space was performed using CREST. In addition, a detailed exploration of TS conformations was performed for the selectivity-determining step (see SI page S33 for details)

Our computational study sought to identify both the turnover-limiting and stereoselectivity-determining steps of the catalytic cycle and to explain the origins of experimentally observed stereoselectivity. The potential energy surface for the lowest energy pathway resulting from our investigation is shown in Figure 3. The reaction is initiated via the coordination of diphenyl phosphine **2a** to Cu-Duphos to give the Cu–$HPPh_2^+$ complex **5aH$^+$**. Deprotonation of this cationic complex **5aH$^+$** by DBU is a low barrier step (**TS$_{Dep}$**, $\Delta G^‡$ = 4.8 kcal/mol) that leads to the reversible formation of Cu-phosphido intermediate **5a** (chosen as the reference structure in the reaction coordinate). Following deprotonation, **5a** binds cyclopropene **1a** via π-coordination transition structure **TS$_{Coord}$** ($\Delta G^‡$ = 15.1 kcal/mol) to generate Cu-alkene complex **Int$_{Coord}$**. The subsequent 1,2-migratory insertion into the cyclopropene π-bond (**TS$_{MI}$**) has a free energy barrier of 19.2 kcal/mol relative to **5a** and represents a highly exothermic step in the pathway, which results in a stable, significantly lower energy copper coordinated cyclopropyl phosphine intermediate **6a** – residing 12.5 kcal/mol below the monomeric resting state **5a**. The reaction pathway then proceeds through a facile stereo-retentive protodemetalation (**TS$_{PDM}$**, $\Delta G^‡$ = -6.3 kcal/mol relative to **5a**) – a copper mediated protonation from DBU occurs syn to the diphenylphosphine substituent – to concomitantly regenerate **4** and afford the *syn*-hydrophosphinated cyclopropene product **3aa** (transferred proton shown in blue).[37-39] This protodemetalation step (**TS$_{PDM}$**) proceeds through a unique three-center, two-electron bond transition structure (C–Cu bond-breaking is 2.11 Å and C–H bond forming distance is 1.42 Å), consistent with the exclusive *syn* addition observed when the reaction is performed with *d*-**2a** (Figure 4 and Figure2C) (vide supra).

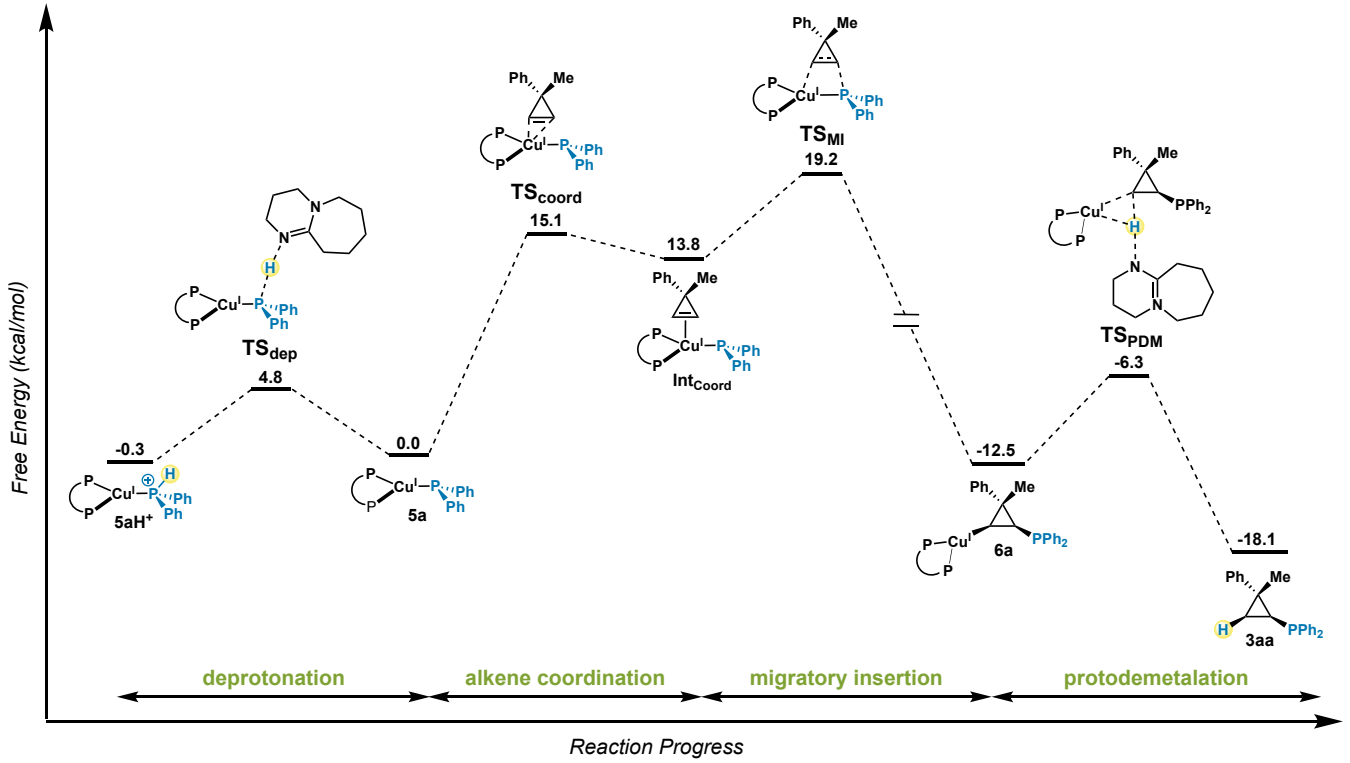

Figure 3. Reaction coordinate diagram depicting the relative barriers of deprotonation, alkene coordination, migratory insertion and protodemetalation in the hydrophosphination of cyclopropene. Migratory insertion is the stereoselectivity determining step.

Incidentally, several alternative pathways for proto-demetalation were also explored computationally (See SI page S34). A *syn*-protodemetalation TS analogous to **TS$_{PDM}$**, whereby copper mediates the proton transfer from a protonated PPh_2 on the adjacent carbon, was found to be 25 kcal/mol higher in energy than **TS$_{PDM}$**.

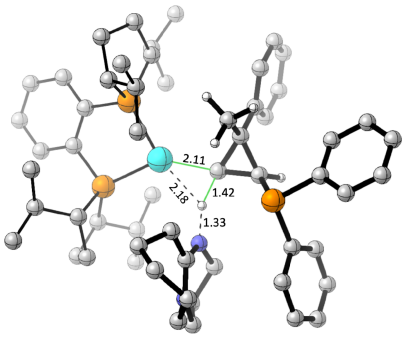

Figure 4. Three-center, two-electron bond transition structure for the product-forming *syn*-protodemetalation of Cu-Duphos from cyclopropene via DBU-H$^+$.

Analysis of the potential energy surface indicates that **TS$_{MI}$** is the enantio- and diastereoselectivity-determining step in the hydrophosphination reaction. To investigate catalyst-substrate interactions that dictate the enantioselectivity in this reaction, a conformational search was conducted on **TS$_{MI}$** for transition structures that lead to the formation of both the major and minor enantiomers of **3aa**. The lowest energy transition structure which leads to the major enantiomer (Figure 5A, **TS$_{MI\text{-}Major}$**) is favored by 2.1 kcal/mol with respect to the lowest energy structure for the minor enantiomer (Figure 5A, **TS$_{MI\text{-}Minor}$**). At 298 K, a $\Delta\Delta G^{\ddagger}$ of 2.1 kcal/mol corresponds to a predicted *er* of 97.5:2.5, which is in excellent agreement with the experimental *er* of 98:2 ($\Delta\Delta G^{\ddagger}$ of 2.3 kcal/mol) for the title reaction.

To further evaluate the origin of enantioselectivity, a distortion-interaction analysis was performed on **TS$_{MI\text{-}Major}$** and **TS$_{MI\text{-}Minor}$**.[40-42] Distortion energy describes the energy required to distort reactants and catalysts from their respective ground states into the necessary transition state conformations. Energy decomposition revealed that the major enantiomer suffers a greater degree of distortion energy, 2.4 kcal/mol ($\Delta\Delta E^{\ddagger}$) more than the minor enantiomer (Figure 5A). The majority (1.8 kcal/mol) of this 2.4 kcal/mol difference in distortion energy arises from the distortion of the diphenyl phosphine and Cu-DuPhos catalyst, while the remaining 0.6 kcal/mol arises from distortion of the cyclopropene substrate. Despite distortion energy favoring the minor enantiomer, advantageous interaction energy favors the major enantiomer by 5.6 kcal/mol. Interaction energy describes how the distorted catalyst and reactant fragments interact with one another within the TS, a portion of this can be accounted for as dispersion energy. The major enantiomer exhibits favorable dispersions in the form of significant CH—π interactions between the diphenylphosphine and the cyclopropene methyl group as well as moderate dispersions amongst the Cu-DuPhos isopropyl groups and the cyclopropene substrate (Figure 5B). A visual comparison of the dispersion interactions in the enantioselectivity-determining transition states shows that **TS$_{MI\text{-}major}$** enjoys more stabilizing dispersion interactions than **TS$_{MI\text{-}minor}$** (as evidenced by the greater green areas in the NCI plots of the two TSs shown in Figure 5B).[43,44] In addition to the favorable dispersions imparted by its isopropyl groups in **TS$_{MI\text{-}}$**

Major, the Cu-DuPhos catalyst also serves to add steric bulk to the catalytic pocket, blocking more than three-fourths of the pocket when coordinated to PPh_2, forcing the cyclopropene substrate to bind in the same location for both enantiomers (see SI page S37).

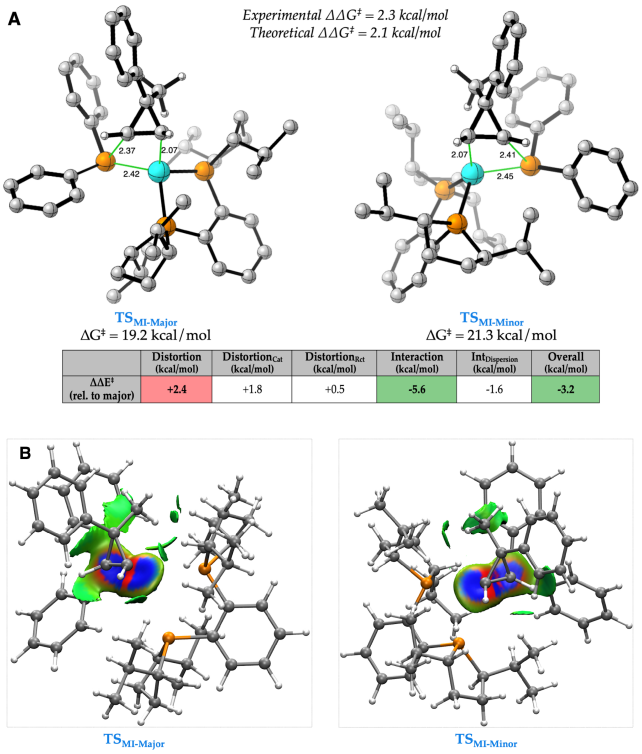

	Distortion (kcal/mol)	$Distortion_{Cat}$ (kcal/mol)	$Distortion_{Rct}$ (kcal/mol)	Interaction (kcal/mol)	$Int_{Dispersion}$ (kcal/mol)	Overall (kcal/mol)
ΔΔE‡ (rel. to major)	+2.4	+1.8	+0.5	-5.6	-1.6	-3.2

Figure 5. (A) Lowest energy TSs of the enantioselectivity-determining step with experimental and theoretical free energy barriers after Boltzmann weighting. Also shown are components of the energy decomposition analysis relative to the major enantiomer. ΔDistortion of the catalyst (Cat) and reactants (Rct) versus overall ΔInteraction (including ΔDispersion) are highlighted. **(B)** Non-covalent interaction (NCI) plots depict dispersive interactions (shown in green) between Cu-DuPhos and PPh_2 with cyclopropene reactants for each TS leading to the major and minor enantiomers of product (Isosurface of 0.009).

From this analysis, steric interactions have been identified to play a key role in controlling stereoselectivity. Using this information, we chose to investigate the buried volume and steric maps for intermediate **5a** with **L1**, **L3**, **L4** and **L5** as ligands.[45-46] The buried volume analysis reveals that ligand **L1** (Figure 6A) has a slightly smaller available free volume compared to the best ligand **L5** (Figure 6C). However, **L5** is more fluctional compared to the rigid biphenyl backbone of **L1**, thereby accommodating the incoming cyclopropene more readily. This leads to an overall reduction in the background reaction of **L5**, compared to **L1**, thus enabling better enantioselectivity in **L5**. Similarly, despite having the same backbone as **L5** (R=^{i}Pr), ligands **L3** (R=Me, Figure 6B) and **L4** (R=Et) have more available free volume, leading to overall poorer steric control and slightly lower enantioselectivity.[47]

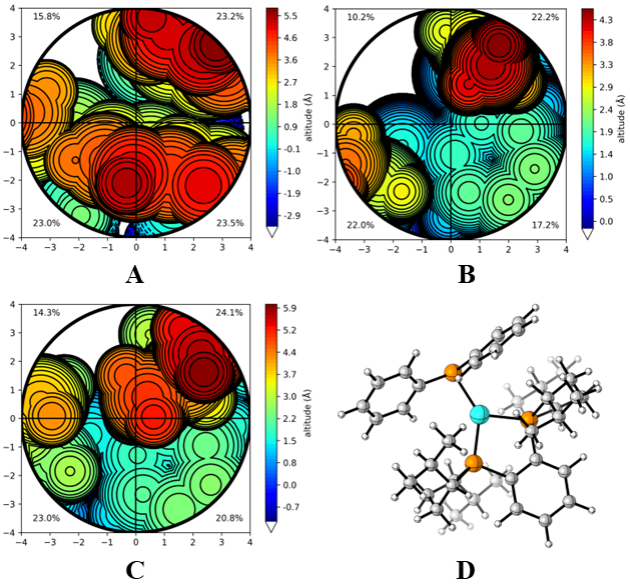

Figure 6. Steric maps depicting the catalytic pocket prior to coordination of cyclopropene when the ligand on copper is **(A)** R-SEGPHOS (**L1**), **(B)** (R,R)-Me-DuPhos (**L3**), or **(C)** (R,R)-^{i}Pr-DuPhos (**L5**). The orientation of the copper-phosphido complexes in these steric maps is depicted in **D**.

In conclusion, we report asymmetric hydrophosphination of cyclopropenes in high enantio- and diastereoselectivities. Mechanistic studies reveal an unusual dimeric resting state and a surprising rate enhancement effect from DBU, which plays an important role in forming the catalytically active monomer. Proof of concept for enrichment of phosphorus stereocenters is demonstrated through a DyKAT of an unsymmetrically substituted secondary phosphine. Both the enantio- and diastereoselectivity of the product is determined during the migratory insertion step. An analysis of the relevant TSs indicate that selectivity is controlled by a combination of dispersion and steric interactions. These insights will guide future studies on developing methods to set phosphorus stereocenters and design both mono- and bidentate phosphine ligands. These studies help advance our understanding of copper catalysis, hydrofunctionalization, and phosphine synthesis.

ASSOCIATED CONTENT

Supporting Information

AUTHOR INFORMATION

Corresponding Authors

Vy M. Dong – Department of Chemistry, University of California, Irvine, Irvine, California 92697, United States; orcid.org/0000-0002-8099-1048; Email: dongv@uci.edu

Jennifer S. Hirschi – Department of Chemistry, Binghamton University, Binghamton, New York 13902, United States; https://orcid.org/0000-0002-3470-0561; Email: jhirschi@binghamton.edu

Shaozhen Nie – Department of Medicinal Chemistry, GSK, 1250 South Collegeville Road, Collegeville, Pennsylvania 19426, United States; Email: shaozhen.x.nie@gsk.com

Authors

Brian S. Daniel − Department of Chemistry, University of California, Irvine, Irvine, California 92697, United States

Xintong Hou − Department of Chemistry, University of California, Irvine, Irvine, California 92697, United States

Stephanie A. Corio – Department of Chemistry, Binghamton University, Binghamton, New York 13902, United States; https://orcid.org/0000-0001-9029-3895

Lindsey M. Weissman – Department of Chemistry, Binghamton University, Binghamton, New York 13902, United States; https://orcid.org/0000-0003-4437-9991

Author Contributions:

‡ Brian S. Daniel and Xintong Hou contributed equally to this work.

Funding Sources

VMD acknowledges the National Science Foundation (CHE-1956457) and National Institutes of Health (R35GM127071). JSH acknowledges the National Institute of General Medicine NIH R35GM147183 as well as the XSEDE Science Gateway Program (under the NSF Grant Numbers ACI-1548562, CHE180061).

Notes

The authors declare no competing financial interest.

ACKNOWLEDGMENT

We thank Solvias AG for donating commercial ligands and phosphine compounds used in the phosphine scope.

REFERENCES

[1] (a) Zhou, Q. L. Privileged Chiral Ligands and Catalysts; Wiley-VCH: Weinheim, Germany, 2011; Vol. 6. (b) Horsman, G. P.; Zechel. D. L. Phosphonate Biochemistry. *Chem. Rev*. **2017**, *117*, 5704−5783. (c) Ni, H.; Chan, W. L.; Lu, Y. Phosphine-Catalyzed Asymmetric Organic Reactions. *Chem. Rev*. **2018**, *118*, 9344−9411. (d) Iaroshenko, V. Organophosphorus Chemistry: from Molecules to Applications. Wiley-VCH: Weinheim, **2019**.

[2] Devreux, V.; Wiesner, J.; Goeman, J. L.; Van der Eycken, J.; Jomaa, H.; Van Calenbergh, S. Synthesis and Biological Evaluation of Cyclopropyl Analogues of Fosmidomycin as Potent *Plasmodium falciparum* Growth Inhibitors. *J. Med. Chem*. **2006**, *49*, 2656−2660.

[3] Suzuki, K.; Hori, Y.; Nakayama, Y.; Kobayashi, T. Development of New Phosphine Ligands (BRIDPs) for Efficient Palladium-Catalyzed Coupling Reactions and Their Application to Industrial Process. *J. Synth. Org. Chem. Jpn*, **2011**, *69*, 1231−1240.

[4] For selected examples of hydrophosphination, see: (a) Wicht, D. K.; Glueck, D. S. Hydrophosphination and Related Reactions. Togni A, Grützmacher H, Eds. Wiley-VCH: Weinheim, **2001**, 143−170. (b) Rosenberg, L. Mechanism of Metal-Catalyzed Hydrophosphination of Alkenes and Alkynes. *ACS Catal*. **2013**, *3*, 2845−2855. (c) Bange, C. A.; Waterman, R. Challenges in Catalytic Hydrophosphination. *Chem. Eur. J*. **2016**, *22*, 12598−12605. (d) Glueck, D. S. Metal-Catalyzed P−C Bond Formation via P−H Oxidative Addition: Fundamentals and Recent Advances. *J. Org. Chem*. **2020**, *85*, 14276−14285. (e) Troev K. D. Reactivity of P−H Group of Phosphines. *Academic Press*, **2018**, 19−144. (f) Belli, R. G.; Yang, J.; Bahena, E, N.; McDonald, R.; Rosenberg, L. Mechanism and Catalyst Design in Ru-Catalyzed Alkene Hydrophosphination. *ACS Catal*. **2022**, *12*, 5247−5262. (g) Novas, B. T.; Waterman, R. Metal-Catalyzed Hydrophosphination. *ChemCatChem*, **2022**, *14*, 1−31. (h) Zhang, Y.; Jiang, Y.; Li, M.; Huang, Z.; Wang, J. Palladium-Catalyzed Diastereo- and Enantioselective Desymmetric Hydrophosphination of Cyclopropenes. *Chem. Cat.* **2022**, *2*, 3163−3173.

[5] Trost, B. M. The Atom Economy−A Search for Synthetic Efficiency. *Science*, **1991**, *254*, 1471−1477.

[6] (a) Pullarkat, S. A.; Leung, P. H. Chiral Metal Complex-Promoted Asymmetric Hydrophosphinations. *Top. Organomet. Chem*. **2013**, *43*, 145−166. (b) Pullarkat, S. A. Recent Progress in Palladium-Catalyzed Asymmetric Hydrophosphination. *Synthesis.* **2016**, *48*, 493−503. (c) Chew, R. J.; Leung, P. H. Our Odyssey with Functionalized Chiral Phosphines: From Optical Resolution to Asymmetric Synthesis to Catalysis. *Chem. Rec*. **2016**, *16*, 141−158.

[7] (a) Join, B.; Mimeau, D.; Delacroix, O.; Gaumont, A. C. Pallado-Catalyzed Hydrophosphination of Alkynes: Access to Enantio-Enriched P-Stereogenic Vinyl Phosphine-Boranes. *Chem. Commun*. **2006**, *30*, 3249−3251. (b) Liu, X. T.; Han, X. Y.; Wu, Y.; Sun, Y. Y.; Gao, L.; Huang, Z.; Zhang, Q. W. Ni-Catalyzed Asymmetric Hydrophosphination of Unactivated Alkynes. *J. Am. Chem. Soc*. **2021**, *143*, 11309−11316.

[8] (a) Sadder, A.; Ong, Y. J.; Kojima, T.; Foo, C. Q.; Li, Y.; Pullarkat, S. A.; Leung, P. H. Desymmetrization of Achiral Heterobicyclic Alkenes through Catalytic Asymmetric Hydrophosphination. *Chem. Asian J.* **2018**. *13*, 2829−2833. (b) Lu, Z.; Zhang, H.; Yang, Z.; Ding, N.; Meng, L.; Wang, J. Asymmetric Hydrophosphination of Heterobicyclic Alkenes: Facile Access to Phosphine Ligands for Asymmetric Catalysis. *ACS Catal*. **2019**, *9*, 1457−1463.

[9] (a) Kovacik, I.; Wicht, D. K.; Grewal, N. S.; Glueck, D. S.; Incarvito, C. D.; Guzei, I. A.; Rheingold, A. L. Pt(Me-Duphos)-Catalyzed Asymmetric Hydrophosphination of Activated Olefins: Enantioselective Synthesis of Chiral Phosphines. *Organometallics* **2000**, *19*, 950−953. (b) Sadow, A. D.; Haller, I.; Fadini, L.; Togni, A. Nickel(II)-Catalyzed Highly Enantioselective Hydrophosphination of Methacrylonitrile. *J. Am. Chem. Soc.* **2004**, *126*, 14704−14705. (c) Feng, J. J.; Chem, X. F.; Shi, M.; Duan, W. L. Palladium-Catalyzed Asymmetric Addition of Diarylphosphines to Enones toward the Synthesis of Chiral Phosphines. *J. Am. Chem. Soc*. **2010**, *132*, 5562−5563. (d) Huang, Y.-H; Pullarkat, S. A.; Li, Y.-X.; Leung, P. H. Palladacycle-Catalyzed Asymmetric Hydrophosphination of Enones for Synthesis of C*- and P*- Chiral Tertiary Phosphines. *Inorg. Chem*. **2012**, *51*, 2533−2540 (e) Chen, Y.-R.; Feng, J.-J.; Duan, W.-L. NHC-Copper-Catalyzed

Asymmetric 1,4-Addition of Diarylphosphines to α,β-Unsaturated Ketones. *Tetrahedron Lett*. **2014**, *55*, 595−597. (f) Teo, R. H. X.; Chen, H. G. J.; Li, Y.-X.; Pullarkat, P. A.; Leung, P. K. Asymmetric Catalytic 1,2-Dihydrophosphination of Secondary 1,2-Diphosphines-Direct Access to Free *P**- and *P**,*C**-Diphosphines. *Adv. Synth. Catal*. **2020**, *362*, 2373−2378. (g) Li, Y.-B.; Tian, H.; Yin, L. Copper(I)-Catalyzed Asymmetric 1,4-Conjugate Hydrophosphination of α,β-Unsaturated Amides. *J. Am. Chem. Soc*. **2020**, *142*, 20098−20106. (h) Yue, W.-J.; Xiao, J.-Z.; Zhang, S.; Yin, L. Rapid Synthesis of Chiral 1,2-Bisphosphine Derivatives through Copper(I)-Catalyzed Asymmetric Conjugate Hydrophosphination. *Angew. Chem. Int. Ed*. **2020**, *59*, 7057−7062. (i) Wang, C.-Y.; Huang, K.-S.; Ye, J.; Duan, W.-L. Asymmetric Synthesis of P-Stereogenic Secondary Phosphine-Boranes by an Unsymmetric Bisphosphine Pincer-Nickel Complex. *J. Am. Chem. Soc*. **2021**, *143*, 5685−5690. (j) Pérez, J. M.; Postolache, R.; Castiñeira Reis, M.; Sinnema, E. G.; Vargová, D.; Vries, F.; Otten, E. Ge, L.; Harutyunyan, S. R. Manganese(I)-Catalyzed H−P Bond Activation via Metal-Ligand Cooperation. *J. Am. Chem. Soc*. **2021**, *143*, 20071−20076. (k) Ge, L.; Harutyunyan, S. R. Manganese(I)-Catalyzed Access to 1,2-Bisphosphine Ligands. *Chem. Sci*., **2022**, *13*, 1307−1312. (l) Zhang, S.; Xiao, J.; Li, Y.; Shi, C.; Yin, L. Copper(I)-Catalyzed Asymmetric Alkylation of Unsymmetrical Secondary Phospines. *J. Am. Chem. Soc.* **2021**, *143*, 9912−9921. (m) Li, Y.; Tian, H.; Zhang, S.; Xiao, J.; Yin, L. Copper(I)-Catalzyed Asymmetric Synthesis of *P*-Chiral Aminophosphinites. *Angew. Chem. Int. Ed.* **2022**, *61*, 2−7.

[10] (a) Bach, R. D.; Dmitrenko, O. Strain Energy of Small Ring Hydrocarbons. Influence of C−H Bond Dissociation Energies. *J. Am. Chem. Soc*. **2004**, *126*, 4444−4452. (b) Wiberg, K. B. The Concept of Strain in Organic Chemistry. *Angew. Chem. Int. Ed*. **1986**, *25*, 312−322.

[11] (a) Demjanov, N. Y.; Doyarenko, M. N. Cyclopropene. *Bull. Acad. Sci. Russ*. **1922**, *16*, 297−304. (b) Carter, F. L.; Frampton, V. L. Review of the Chemistry of Cyclopropene Compounds. *Chem. Rev*. **1964**, *64*, 497−525. (c) Closs, G. L. Cyclopropenes. *Adv. Alicyclic Chem*. **1966**, *1*, 53−127. (d) Baird, M. S. Thermally Induced Cyclopropene-Carbene Rearrangements: An Overview. *Chem. Rev*. **2003**, *103*, 1271−1294. (e) Walsh, R. The cyclopropene Pyrolysis Story. *Chem. Soc. Rev*. **2005**, *34*, 714−732. (f) Rubin, M.; Rubina, M.; Gevorgyan, V. Recent Advances in Cyclopropene Chemistry. *Synthesis.* **2006**, *2006*, 1221−1245. (g) Rubin, M.; Rubina, M.; Gevorgyan, V. Transition Metal Chemistry of Cyclopropenes and Cyclopropanes. *Chem. Rev*. **2007**, *107*, 3117−3179. (h) Zhu, Z.-B.; Wei, Y.; Shi, M. Recent Developments of Cyclopropene Chemistry. *Chem. Soc. Rev*. **2011**, *40*, 5534−5563. (i) Vicente, R. Recent Progresses towards the Strengthening of Cyclopropene Chemistry. *Synthesis.* **2016**, *48*, 2343−2360. (j) Raiguru, B. P.; Nayak, S.; Mishra, D. R.; Das, T.; Mohapatra, S.; Mishra, N. P. Synthetic Applications of Cyclopropene and Cyclopropenone: Recent Progress and Developments. *Asian J. Org. Chem*. **2020**, *9*, 1088−1132. (k) Li, P.-H.; Zhang, X.-Y.; Shi, M. Recent Developments in Cyclopropene Chemistry. *Chem. Commun*. **2020**, *56*, 5457−5471. (l) Cohen, Y.; Marek, I. Regio- and Diastereoselective Copper-Catalyzed Carbometallation of Cyclopropenylsilanes. *Org. Lett*. **2019**, *21*, 9162−9165.

[12] For selected examples for hydrofunctionalization of cyclopropenes, see: (a) Dian, L.-Y.; Marek, I. Asymmetric Preparation of Polysubstituted Cyclopropanes Based on Direct Functionalization of Achiral Three-Membered Carbocycles. *Chem. Rev*. **2018**, *118*, 8415−8434. (b) Rubina, M.; Rubin, M.; Gevorgyan, V. Catalytic Enantioselective Hydroboration of Cyclopropenes. *J. Am. Chem. Soc*. **2003**, *125*, 7198−7199. (c) Rubina, M.; Rubin, M.; Gevorgyan, V. Catalytic Enantioselective Hydrostannation of Cyclopropenes. *J. Am. Chem. Soc*. **2004**, *126*, 3688−3689. (d) Sherrill, W. M.; Rubin, M. Rhodium-Catalyzed Hydroformylation of Cyclopropenes. *J. Am. Chem. Soc*. **2008**, *130*, 13804−13809. (e) Phan, D. H. T.; Kou, K. G. M.; Dong, V. M. Enantioselective Desymmetrization of Cyclopropenes by Hydroacylation. *J. Am. Chem. Soc*. **2010**, *132*, 16354−16355. (f) Liu, F.; Bugaut, X.; Schedler, M.; Fröhlich, R.; Glorius, F. Designing N-Heterocyclic Carbenes: Simultaneous Enhancement of Reactivity and Enantioselectivity in the Asymmetric Hydroacylation of Cyclopropenes. *Angew. Chem. Int. Ed*. **2011**, *50*, 12626−12630. (g) Teng, H.-L.; Luo, Y.; Wang, B.; Zhang, L.; Nishiura, M.; Hou, Z. Synthesis of Chiral Aminocyclopropanes by Rare-Earth-Metal Catalyzed Cyclopropene Hydroamination. *Angew. Chem. Int. Ed*. **2016**, *55*, 15406−15410. (h) Parra, A.; Amenós, L.; Guisán-Ceinos, M.; López, A.; Ruano, J. L. G.; Tortosa, M. Copper-Catalyzed Diastereo- and Enantioselective Desymmetrization of Cyclopropenes: Synthesis of Cyclopropylboronates. *J. Am. Chem. Soc*. **2014**, *136*, 15833−15836. (i) Li, Z.; Zhao, J.; Sun, B.; Zhou, T.; Liu, M.; Liu, S.; Zhang, M.; Zhang, Q. Asymmetric Nitrone Synthesis via Ligand-Enabled Copper-Catalyzed Cope-Type Hydroamination of Cyclopropene with Oxime. *J. Am. Chem. Soc*. **2017**, *139*, 11702−11705. (j) Luo, Y.; Teng, H.-L.; Nishiura, M.; Hou, Z. Asymmetric Yttrium-Catalyzed C(sp^3)−H Addition of 2-Methyl Azaarenes to Cyclopropenes. *Angew. Chem. Int. Ed*. **2017**, *56*, 9207−9210. (k) Dian, L.; Marek, I. Rhodium-Catalyzed Arylation of Cyclopropenes Based on Asymmetric Direct Functionalization of Three Membered Carbocycles. *Angew. Chem. Int. Ed*. **2018**, *57*, 3682−3686. (l) Zhang, H.; Huang, W.; Wang, T.; Meng, F.-K. Cobalt Catalyzed Diastereo- and Enantioselective Hydroalkenylation of Cyclopropenes with Alkenylboronic Acids. *Angew. Chem. Int. Ed*. **2019**, *58*, 11049−11053. (m) Zheng, G.-F.; Zhou, Z.; Zhu, G.-X.; Zhai, S.-L.; Xu, H.-Y.; Duan, X.-J.; Yi, W.; Li, X.-W. Rhodium(III)-Catalyzed Enantio- and Diastereoselective C−H Cyclopropylation of N-Phenoxylsulfonamides: Combined Experimental and Computational Studies. *Angew. Chem. Int. Ed*. **2020**, *59*, 2890−2896 (n) Huang, W.; Meng, F.-K. Cobalt-Catalyzed Diastereo- and Enantioselective Hydroalkylation of Cyclopropenes with Cobalt Homoenolates. *Angew. Chem. Int. Ed*. **2021**, *59*, 2694−2698. (o) Dian, L.; Marek, I. Cobalt-Catalyzed Diastereoselective and Enantioselective Hydrosilylation of Achiral Cyclopropenes. *Org. Lett*. **2020**, *22*, 4914−4918. (p) Nie, S.-Z.; Lu, A.; Kuker, E. L.; Dong, V. M. Enantioselective Hydrothiolation: Diverging Cyclopropenes through Ligand Control. *J. Am. Chem. Soc*. **2021**, *143*, 6176−6184. (q) Yu, R.; Cai, S.-Z.; Li, C.; Fang, X. Nickel-Catalyzed Asymmetric Hydroaryloxy- and Hydroalkoxycarbonylation of Cyclopropenes. *Angew. Chem. Int. Ed*. **2022**, *61*, 1−7. (r) Huang, Q.; Chen, Y.; Zhou, X.; Dai, L.; Lu Y. Nickel-Hydride-Catalyzed Diastereo- and Enantioselective Hydroalkylation of Cyclopropenes. *Angew. Chem. Int. Ed.,* **2022**, *61*, 1−6.

[13] Li, J-N.; Liu, L.; Fu, Y.; Guo, Q.-X. What are the pKa Values of Organophosphorus Compounds? *Tetrahedron.* **2006**, *62*, 4453−4462.

[14] (a) Han, L.-B.; Zhao, C.-Q.; Onozawa, S.; Goto, M.; Tanaka, M. Retention of Configuration on the Oxidative Addition of P−H Bond to Platinum(0) Complexes: the First Straightforward Synthesis of Enantiomerically Pure P-chiral Alkenylphosphinates via Palladium-Catalyzed Stereospecific Hydrophosphinylation of Alkynes. *J. Am. Chem. Soc*. **2002**, *124*, 3842−3843. (b) Xu, Q.; Han, L.-B. Palladium-Catalyzed Asymmetric Hydrophosphorylation of Norbornenes. *Org. Lett*., **2006**, *8*, 2099−2101. (c) Beaud, R.; Phipps, R. J.; Gaunt, M. J. Enantioselective Cu-Catalyzed Arylation of Secondary Phosphine Oxides with Diaryliodonium Salts toward the Synthesis of P-Chiral Phosphines. *J. Am. Chem. Soc*. **2016**, *138*, 13183−13186. (d) Nie, S.-Z.; Davison, R. T.; Dong, V. M. Enantioselective Coupling of Dienes and Phosphine Oxides. *J. Am. Chem. Soc*. **2018**, *140*, 16450−16454. (e) Trost, B. M.; Spohr, S. M.; Rolka, A. B.; Kalnmals, C. A. Desymmetrization of Phosphinic Acids via Pd-Catalyzed Asymmetric Allylic Alkylation: Rapid Access to *P*-chiral Phosphinates. *J. Am. Chem. Soc*. **2019**, *141*, 14098−14103. (f) Yang, Z.; Gu, X.; Han, L.-B.; Wang, J. Palladium-Catalyzed Asymmetric Hydrophosphorylation of Alkynes: Facile Access to P-Stereogenic Phosphinates. *Chem. Sci*. **2020**, *11*, 7451−7455. (g) Dai, Q.; Liu, L.; Qian, Y.; Li, W.; Zhang, J.-L. Construction of P-Chiral Alkenylphosphine Oxides through Highly

Chemo-, Regio-, and Enantioselective Hydrophosphinylation of Alkynes. *Angew. Chem. Int. Ed*. **2020**, *59*, 20645−20650. (h) Yang, Z.; Wang, J. Enantioselective Palladium-Catalyzed Hydrophosphinylation of Allenes with Phosphine Oxides: Access to Chiral Allylic Phosphine Oxides. *Angew. Chem. Int. Ed*. **2021**, *60*, 27288−27292. (i) Zhang, Q.; Liu, X.-T.; Wu, Y.; Zhang, Q.-W. Ni-Catalyzed Enantioselective Allylic Alkylation of *H*-Phosphinates. *Org. Lett*. **2021**, *23*, 8683−8687. (j) Li, B.; Liu, M.; Rehman, S. U.; Li, C. Rh-Catalyzed Regio- and Enantioselective Allylic Phosphinylation. *J. Am. Chem. Soc*. **2022**, *144*, 2893−2898. (k) Wang, H.; Qian, H.; Zhang, J.; Ma, S. Catalytic Asymmetric Axially Chiral Allenyl C−P Bond Formation. *J. Am. Chem. Soc*. **2022**, *144*, 12619−12626. (l) Alnasleh, B. K.; Sherrill, W. M.; Rubin, M. Palladium-Catalyzed Hydrophosphorylation and Hydrophosphinylation of Cyclopropenes. *Org. Lett*., **2008**, *10*, 3231−3234.

[15] For selected example of metal-phosphido chemistry, see: (a) Fortman, G. C.; Slawin, A. M. Z.; Nolan, S. P. A Versatile Cuprous Synthon: [Cu(IPr)(OH)] (IPr = 1,3 bis(diisopropylphenyl)imidazol-2-ylidene). *Organometallics.* **2010**, *29*, 3966−3972. (b) Najafabadi, B. K.; Corrigan, J. F. Enhanced Thermal Stability of Cu-Silylphosphido Complexes *via* NHC Ligation. *Dalton Trans*. **2015**, *44*, 14235−14241. (c) Wang, G.; Gibbons, S. K.; Glueck, D. S.; Sibbald, C.; Fleming, J. T.; Higham, L. J.; Rheingold, A. L. Copper−Phosphido Intermediates in Cu(IPr)-Catalyzed Synthesis of 1-Phosphapyracenes via Tandem Alkylation/Arylation of Primary Phosphines. *Organometallics.* **2018**, *37*, 1760−1772. (d) Gibbons, S. K.; Valleau, C. R. D.; Peltier, J. L.; Cain, M. F.; Hughes, R. P.; Glueck, D. S.; Golen, J. A.; Rheingold, A. L. Diastereoselective Coordination of P-Stereogenic Secondary Phosphines in Copper(I) Chiral Bis(phosphine) Complexes: Structure, Dynamics, and Generation of Phosphido Complexes. *Inorg. Chem*. **2019**, *58*, 8854−8865. (e) Gallant, S. K.; Tipker, R. M.; Glueck, D. S. Copper-Catalyzed Asymmetric Alkylation of Secondary Phosphines via Rapid Pyramidal Inversion in P-Stereogenic Cu-Phosphido Intermediates. *Organometallics*. **2022**, *41*, 1721−1730. (f) Moncarz, J. R.; Laritcheva, N. F.; Glueck, D. S. Palladium-Catalyzed Asymmetric Phosphination: Enantioselective Synthesis of a P-Chirogenic Phosphine. *J. Am. Chem. Soc.* **2002**, *124*, 13356−13357. (g) Blank, N. F.; Moncarz, J. R.; Brunker, T. J.; Scriban, C.; Anderson, B. J.; Amir, O.; Glueck, D, S.; Zakharov, L. N.; Golen, J. A.; Incarvito, C. D.; Rheingold, A. L. Palladium-Catalyzed Asymmetric Phosphination. Scope, Mechanism, and Origin of Enantioselectivity. *J. Am. Chem. Soc*. **2007**, *129*, 6847−6858. (h) Chan, V. S.; Stewart, I. C.; Bergman, R. G.; Toste, F. D. Asymmetric Catalytic Synthesis of *P*-Stereogenic Phosphines via a Nucleophilic Ruthenium Phosphido Complex. *J. Am. Chem. Soc*. **2006**, *128*, 2786−2787. (i) Chan, V. S.; Bergman, R. G.; Toste, F. D. Pd-Catalyzed Dynamic Kinetic Enantioselective Arylation of Silylphosphines. *J. Am. Chem. Soc*. **2007**, *129*, 15122−15123. (j) Chan, V. S.; Chiu, M.; Bergman, R. G.; Toste, F. D. Development of Ruthenium Catalyts for the Enantioselective Synthesis of P-Stereogenic Phosphines via Nucleophilic Phosphido Intermediates. *J. Am. Chem. Soc*. **2009**, *131*, 6021−6032. (k) Yang, Q.; Zhou, J.; Wang, Jun. Enantioselective Copper-Catalyzed Hydrophosphination of Alkenyl Isoquinolines. *Chem. Sci.* **2023**. DOI: 10.1039/D2SC06950D.

[16] Li, Z.-Y.; Peng, G.-C.; Zhao, J.-B.; Zhang, Q. Catalytically Generated Allyl Cu(I) Intermediate via Cyclopropene Ring-Opening Coupling en Route to Allylphosphonates. *Org. Lett*. **2016**, *18*, 4840−4843.

[17] Torborg, C.; Beller, M. Recent Application of Palladium-Catalyzed Coupling Reactions in the Pharmaceutical, Agrochemical, and Fine Chemical Industries. *Adv. Synth. Catal.* **2009**, *351*, 3027−3043.

[18] (a) Bullock, R. M.; Chen, J. G.; Gagliardi, L.; Chirik, P. J.; Farha, O. K.; Hendon, C. H.; Jones, C. W.; Keith, J. A.; Klosin, J.; Minteer, S. D.; Morris, R. H.; Radosevich, A. T.; Rauchfuss, T. B.; Strotman, N. A.; Vojvodic, A.; Ward, T. R.; Yang, J. Y.; Surendranath, Y. Using Nature's Blueprint to Expand Catalysis with Earth-abundant Metals. *Science*, **2020**, *786*, 1−10. (b) Chen, J.; Lu, Zhan. Asymmetric Hydrofunctionalization of Minimally Functionalized Alkenes via Earth Abundant Transition Metal Catalysis. *Org. Chem. Front.* **2018**, *5*, 160−272. (c) Toutov, A. A.; Liu, W.; Betz, K. N.; Fedorov, A.; Stoltz, B. M.; Grubbs, R. H. Silylatio of C−H Bonds in Aromatic Heterocycles by an Earth-Abundant Metal Catalysis. *Nature*, **2015**, *518*, 80−84.

[19] Deposition number 2100976 for **3aa** and 2154097 for **3la**, contains the supplementary crystallographic data for this paper. These data are provided free of charge by the joint Cambridge Crystallographic Data Centre and Fachinformationszentrum Karlsruhe Access Structures service www.ccdc.cam.ac.uk/structures. The absolute configurations of the remaining cyclopropyl phosphine sulfides **3** are assigned by analogy.

[20] Xu, P.-W.; Yu, J.-S.; Chen, C.; Cao, Z.-Y.; Zhou, F.; Zhou, J. Catalytic Enantioselective Construction of Spiro Quaternary Carbon Stereocenters. *ACS Catal*. **2019**, *9*, 1820−1882.

[21] Rios, R. Enantioselective methodologies for the synthesis of spiro compounds. *Chem. Soc. Rev*. **2012**, *41*, 1060−1074.

[22] (a) Edwards, A.; Rubina, M.; Rubin, M. Nucleophilic Addition of Cyclopropenes. *Curr. Org. Chem*. **2016**, *20*, 1862−1877. (b) Fox, J. M.; Yan, N. Metal Mediated and Catalyzed Nucleophilic Additions to Cyclopropenes. *Curr. Org. Chem*., **2005**, *9*, 719−732. (c) Alnasleh, B. M.; Sherrill, W. M. Rubina, M.; Banning, J.; Rubin, M. Highly Diaostereoselective Formal Nucleophilic Substitution of Bromocyclopropanes. *J. Am. Chem. Soc*. **2009**, *131*, 6906−6907.

[23] (a) Ananikov, V. P.; and Beletskaya, I. P. Alkyne Insertion into the M−P and M−H Bonds (M = Pd, Ni, Pt, and Rh): A Theoretical Mechanistic Study of the C-P and C-H Bond Formation Steps. *Chem. Asian J*. **2011**, *6*, 1423−1430. (b) Burton, K. M. E.; Pantazis, D. A.; Belli, R. G.; McDonald, R.; Rosenberg, L. Alkene Insertion into a Ru-PR_2 Bond. *Organometallics* **2016**, *35*, 3970−3980.

[24] Bures, J. A Simple Graphical Method to Determine the Order in Catalyst. *Angew. Chem. Int. Ed.* **2016**, *55*, 2028−2031.

[25] Zall, C. M.; Linehan, J. C.; Appel, A. M. Triphosphine-Ligated Copper Hydrides for CO_2 Hydrogenation: Structure, Reactivity, and Thermodynamic Studies. *J. Am. Chem. Soc*. **2016**, *138*, 9968−9977.

[26] Yamamoto, Y. Theoretical Study of the Copper-Catalyzed Hydroarylation of (Trifluoromethyl)alkyne with Phenylboronic Acid. *J. Org. Chem*. **2018**, *83*, 12775−12783

[27] Steinreiber, J.; Faber, K.; Griengl. H. De-racemization of Enantiomers versus De-epimerization of Diastereomers−Classification of Dynamic Kinetic Asymmetric Transformation (DYKAT). *Chem. Eur. J*. **2008**, *14*, 8060−8072.

[28] Buhro, W. E.; Zwick, B. D.; Georgiou, S.; Hutchinson, J. P.; Gladysz, J. A. Synthesis, Structure, Dynamic Behavior, and Reactivity of Rhenium Phosphido Complexes (η^5-C_2H_5)Re(NO)(PPh_3)(PR_2): The "Gauche Effect" in Transition-Metal Chemistry. *J. Am. Chem. Soc*. **1988**, *110*, 2427−2439.

[29] Chai, J. D.; Head-Gordon, M. Long-range corrected hybrid density functionals with damped atom-atom dispersion corrections. *Phys. Chem. Chem. Phys.* **2008**, *10*, 6615-6620.

[30] Grimme, S. Semiempirical GGA-type density functional constructed with a long-range dispersion correction. *J. Comput. Chem.* **2006**, *27*, 1787-1799.

[31] Becke, A. Density-Functional Thermochemistry. V. Systematic Optimization of Exchange-Correlation Functionals. *J. Chem. Phys.* **1997**, *107*, 8554-8560.

[32] Weigend, F.; Ahlrichs, R. Balanced basis sets of split valence, triple zeta valence and quadruple zeta valence quality for H to Rn: Design and assessment of accuracy. *Phys. Chem. Chem. Phys.* **2005**, *7*, 3297-3305.

[33] Miertus, S.; Scrocco, E.; Tomasi, J. Electrostatic Interaction of a Solute with a Continuum - a Direct Utilization of Abinitio Molecular Potentials for the Prevision of Solvent Effects. *Chem. Phys.* **1981**, *55*, 117-129.

[34] Tomasi, J.; Mennucci, B.; Cammi, R. Quantum mechanical continuum solvation models. *Chem. Rev.* **2005**, *105*, 2999-3093.

[35] Frisch, M. J.; Trucks, G. W.; Schlegel, H. B.; Scuseria, G. E.; Robb, M. A.; Cheeseman, J. R.; Scalmani, G.; Barone, V.; Petersson, G. A.; Nakatsuji, H.; Li, X.; Caricato, M.; Marenich, A. V.; Bloino, J.; Janesko, B. G.; Gomperts, R.; Mennucci, B.; Hratchian, H. P.; Ortiz, J. V.; Izmaylov, A. F.; Sonnenberg, J. L.; Williams; Ding, F.; Lipparini, F.; Egidi, F.; Goings, J.; Peng, B.; Petrone, A.; Henderson, T.; Ranasinghe, D.; Zakrzewski, V. G.; Gao, J.; Rega, N.; Zheng, G.; Liang, W.; Hada, M.; Ehara, M.; Toyota, K.; Fukuda, R.; Hasegawa, J.; Ishida, M.; Nakajima, T.; Honda, Y.; Kitao, O.; Nakai, H.; Vreven, T.; Throssell, K.; Montgomery, J. A., Jr.; Peralta, J. E.; Ogliaro, F.; Bearpark, M. J.; Heyd, J. J.; Brothers, E. N.; Kudin, K. N.; Staroverov, V. N.; Keith, T. A.; Kobayashi, R.; Normand, J.; Raghavachari, K.; Rendell, A. P.; Burant, J. C.; Iyengar, S. S.; Tomasi, J.; Cossi, M.; Millam, J. M.; Klene, M.; Adamo, C.; Cammi, R.; Ochterski, J. W.; Martin, R. L.; Morokuma, K.; Farkas, O.; Foresman, J. B.; Fox, D. J. *Gaussian 16*; Rev. C.01: Wallingford, CT, 2016.

[36] Ribeiro, R. F.; Marenich, A. V.; Cramer, C. J.; Truhlar, D. G. Use of solution-phase vibrational frequencies in continuum models for the free energy of solvation. *J. Phys. Chem. B* **2011**, *115*, 14556-14562.

[37] O'Duill, M. L.; Engle, K. M. Protodepalladation as a Strategic Elementary Step in Catalysis. *Synthesis*, **2018**, *50,* 4699-4714.

Table of Contents

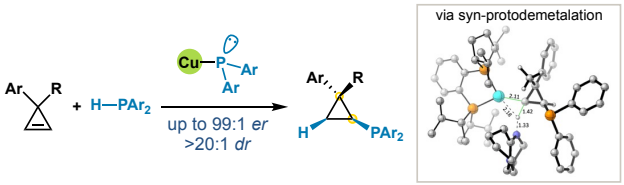

[38] Yao, Y.; Zhang, X.; Ma, S. DFT study on the E-stereoselective reductive A^3-coupling reaction of terminal alkynes with aldehydes and 3-pyrroline. *Org. Chem. Front.*, **2020.** 7, 2047-2054.

[39] Yuan, X.; Wang, S.; Jiang, Y.; Liu, P.; Bi, S. Distinctive mechanistic scenarios and substituent effects of gold(I) versus copper(I) catalysis for hydroacylation of terminal alkynes with glyoxal derivatives. *J. Am. Chem. Soc.* **2022**. 87 (17), 11681-11692.

[40] Bickelhaupt, F. M.; Houk, K. N., Analyzing Reaction Rates with the Distortion/Interaction-Activation Strain Model. *Angew. Chem. Int. Ed. Engl.* **2017,** *56* (34), 10070-10086.

[41] Ess, D. H.; Houk, K. N., Distortion/interaction energy control of 1,3-dipolar cycloaddition reactivity. *J. Am. Chem. Soc.* **2007,** *129* (35), 10646-7.

[42] Maji, R.; Mallojjala, S. C.; Wheeler, S. E., Chiral phosphoric acid catalysis: from numbers to insights. *Chem. Soc. Rev.* **2018,** *47* (4), 1142-1158

[43] Lu, T.; Chen, Q., Independent gradient model based on Hirshfeld partition: A new method for visual study of interactions in chemical systems. *J. Comput. Chem.* **2022,** *43* (8), 539-555.

[44] Lu, T.; Chen, F. Multiwfn: A multifunctional wavefunction analyzer. *J. Comput. Chem*. **2011**, *33* (5), 580-592.

[45] Falivene, L., Cao, Z., Petta, A.; Serra, L.; Poater, A.; Oliva, R.; Scarano, V.; Cavallo, L. Towards the online computer-aided design of catalytic pockets. *Nat. Chem.* **2019**, 11, 872-879.

[46] Schaefer, A. J., Ingman, V. M., Wheeler, S. E. SEQCROW: A ChimeraX bundle to facilitate quantum chemical applications to complex molecular systems. *J. Comput. Chem*. **2021**, *42* (24), 1750-1754.

[47] There is little difference between the buried volumes of L3 and L4, corresponding with the little difference in the observed ee for L3 and L4 (see Supplementary Information Table S2 for buried volumes and all steric maps).